Conformational Instability of Rodlike Polyelectrolytes due to Counterion Fluctuations

Ramin Golestanian

Institute for Advanced Studies in Basic Sciences, Zanjan 45195-159, Iran
and Institute for Studies in Theoretical Physics and Mathematics, P.O. Box 19395-5531, Tehran, Iran

Tanniemola B. Liverpool

Condensed Matter Theory Group, Blackett Laboratory, Imperial College, London SW7 2BZ, UK

(February 1, 2008)

The effective elasticity of highly charged stiff polyelectrolytes is studied in the presence of counterions, with and without added salt. The rigid polymer conformations may become unstable due to an effective attraction induced by counterion density fluctuations. Instabilities at the longest, or intermediate length scales may signal collapse to globule, or necklace states, respectively. In the presence of added-salt, a generalized electrostatic persistence length is obtained, which has a non-trivial dependence on the Debye screening length. It is also found that the onset of conformational instability is a re-entrant phenomenon as a function of polyelectrolyte length for the unscreened case, and the Debye length or salt concentration for the screened case. This may be relevant in understanding the experimentally observed re-entrant condensation of DNA.

I. INTRODUCTION AND SUMMARY

A polyelectrolyte (PE) is an ionic polymer which when dissolved in polar solvents dissociates into a long polymer chain (macroion), and small mobile *counterions*. Because of the electrostatic repulsion of the uncompensated charges on the polymer, the chain is stretched out to rodlike conformations. Naively, one may expect that higher charges on the polyelectrolyte lead to more rodlike configurations. This is not the case, as the tendency towards extended shapes is opposed by stronger attraction to the counterions. The latter may condense on a highly charged polyelectrolyte, giving it a much lower apparent charge [1,2], and resulting in a lower stiffness. Nonetheless, in a mean-field (Poisson-Boltzmann) treatment of the counterions, the conformation of the polyelectrolyte is stretched [3,4].

On the other hand, it is now well known from experiments [5,6], simulations [7], and analytical theories [8–10], that highly charged flexible polyelectrolytes (such as polystyrene sulphonate) can collapse in the presence of multivalent counterions to highly compact states. Stiff polyelectrolytes (such as DNA) could also collapse [11], and rodlike polyelectrolytes may form bundles [12–14], under similar conditions. To account for these effects, an attractive interaction capable of competing with the residual coulomb repulsion (of the polyelectrolyte backbones with compensated charge densities) is needed. Note that the situation is more subtle for stiff polyelectrolytes due to their intrinsic rigidity [15,16,18–20].

To understand the origin of the attractive interaction, consider two like-charged substrates on which counterions are condensed. As the two objects approach each other, the counterions may rearrange their positions. Any *correlated separation of charges* now leads to an *attraction* whose range is of the order of the "correlation hole" of the counterions on each substrate. Several different mechanisms may lead to correlated charge separation: (i) At low temperatures, the counterions form a Wigner crystal on the charged substrate, which leads to an attractive interaction with a range set by the lattice spacing [21–25]. (ii) Specific binding of counterions to the substrate is another mechanism for charge separation [26]. In this case the periodicity, and hence the range of the attraction, is dictated by the underlying structure of the substrate, such as the double helical structure of DNA along which the charged phosphate groups are located. (iii) Thermal fluctuations can also induce instantaneous charge separations which inter-correlate on the two objects, leading to an attraction similar to the van der Waals interaction. Since the dominant fluctuations have wavelengths of the order of the separation of the objects, the range of the attraction is set by the distance between them; i.e. the interaction is long-ranged [2,3,22,27–29]. (iv) Finally, it has been proposed that macroions can be overcharged by the condensing counterions due to the gain in correlation energy [30]. Consequently, when two such macroions are brought close to each other in a neutralizing solution, the distribution of the counterions can be asymmetric leading, at each instant, to one overcharged and one undercharged macroion [31,32]. This mechanism will lead to instantaneous ordinary long-ranged Coulomb attraction between the two decorated macroions, and is reminiscent of covalent bonding in atomic systems in that the macroions are effectively sharing a fraction of their condensed counterions [32].

As thermal fluctuations clearly set the energy scale for the relevance of these different attractive interactions, one may naturally ask the following question [33,34]: Is room temperature 'high' or 'low' for DNA or actin condensation, or bundle formation? In regards to this ques-

tion one should note that although an actual Wigner crystal may appear far–fetched on the surface of DNA or actin at room temperature, remnants of such a structure may survive for multivalent counterions.

Since it is just the local charge separation that is needed for the 'zero temperature' mechanism, and not the long-range order of the global structure, a liquid phase should still lead to attraction provided that some short-range order persists. Consequently, it seems that both types of interactions are in effect at room temperature and the dominant mechanism should be determined by comparing the range of the interaction and the distance between macroions. While the short-ranged interactions seem to play the dominant role in bundle formation [21–26,28], there seems to be a consensus that they are not capable of actually collapsing a single DNA or actin chain [16,17], and thus the long-ranged interaction caused by thermal fluctuations may be responsible for the observed condensation [11,18].

In this paper, we focus on the long wavelength behavior of polyelectrolytes. Our approach is complementary to that of the "Wigner liquid" theories [16,17], whose local formulation corresponds to examination of short wavelength behavior. They find that the softening contribution to the persistence length due to the Wigner liquid correlations is not large enough to fully compensate the mechanical stiffness and render a null persistence length, which would trigger chain collapse. We also find that the softening contribution to the rigidity due to charge fluctuations at the smallest length-scales is never strong enough to completely negate the bare bending rigidity, and obtain collapse *at these scales*, but rather that the 'collapse' occurs at higher length-scales due to *longer* wavelength charge fluctuations. Additional correlations at short length-scales as might be obtained with a Wigner liquid should not affect the large-scale behavior which is the domain of our theory.

To this end, we employ path integral methods [29,35] to study the energy cost of deforming a stiff and highly charged polyelectrolyte in the presence of thermally fluctuating counterions [18]. In particular, consider a chain of length L, with a microscopic persistence length ℓ_p, and average separation a between charges on its backbone, in a neutralizing solution of counterions of valence z. The polyelectrolyte is considered highly charged when a is less than the Bjerrum length $\ell_B = e^2/\epsilon k_B T$, where ϵ is the dielectric constant of the solvent. (For water at room temperature, $\ell_B \simeq 7.1 \mathring{A}$.) We calculate the effective free energy of a fluctuating polyelectrolyte as a perturbative expansion in the deformations around an average rodlike structure. The linear stability of this structure is controlled by a spectrum $\mathcal{E}(k)$, as a function of the deformation wave vector k. A negative value of $\mathcal{E}(k)$ signals an instability at the corresponding wavelength, leading to phase diagrams as in Figs. 2 and 3. In particular, both in the presence of salt and in salt-free conditions, (see Figs. 2 and 3), we find that counterion fluctuations *cannot* trigger collapse of a stiff polyelectrolyte, *unless it*

has a microscopic persistence length less than a critical value of

$$\ell_p^c = \Delta_i \times a \times z^4 \times \left(\frac{\ell_B}{a}\right)^3 \times \left(1 - \frac{a}{z\ell_B}\right)^2. \quad (1)$$

The index i refers to either added-salt (as) or salt-free (sf) conditions, with corresponding numerical constants Δ_{as} and Δ_{sf} which are given later. For $\ell_p < \ell_p^c$, there is a finite domain of intermediate polyelectrolyte lengths L, for which a collapsed conformation is favored.

For a low concentration of added salt, we find an effective persistence length of

$$L_p = \ell_p + \frac{a\,(a/\ell_B)^3}{16z^4\left(1 - \frac{a}{z\ell_B}\right)^2 (\kappa a)^2 \ln^2\left(\frac{1}{\kappa a}\right)} - \frac{c_2}{2\kappa \ln\left(\frac{1}{\kappa a}\right)}, \quad (2)$$

where κ^{-1} is the Debye screening length, related to the salt (number) density n via $\kappa^2 = 4\pi\ell_B n$, and c_2 is a numerical constant given below. The above expression, which is a *non-trivial* generalization of the Odijk-Skolnick-Fixman (OSF) electrostatic persistence length [36], is a sum of repulsive (+) and attractive (-) electrostatic contributions. It can therefore be negative under certain conditions, which we take as an indication of a conformational instability of the rodlike polyelectrolyte (tendency to collapse). This occurs in the regions of the phase diagram indicated in Fig. 3, and only for persistence lengths less than a critical value given by Eq. (1) above. A similar 'softening' contribution to the rigidity and an associated conformational instability, can also be obtained for charged membranes [37]. There are related instabilities caused by surface fluctuation–induced interactions between stiff polymers on membranes [38].

We also find that the onset of conformational instability is a re-entrant phenomenon as a function of polyelectrolyte length for the unscreened case, and the Debye length or salt concentration for the screened case. This may be relevant in understanding the re-entrant condensation of DNA that has been observed experimentally [39], but note that alternative explanations for this phenomenon also exist in the literature [40].

II. THE MODEL

We consider a polyelectrolyte oriented along the x-axis, and parameterize is transverse deviations from a straight line by a two component vector $\mathbf{r}(x)$. By assuming a single valued function $\mathbf{r}(x)$, we implicitly neglect overhangs and knots, as sketched in Fig. 1. The embedding of the polyelectrolyte in space is thus described by the three component vector $\vec{R}(x) = (x, \mathbf{r}(x))$. For each conformation of the polyelectrolyte, we would like to calculate a constrained partition function $\mathcal{Z}[\vec{R}]$, by integrating over

all possible configurations of the counterions in the solution. We do this by using a phenomenological model, which generalizes previous work by Ha and Liu [28] (and is referred to as the Ha-Liu model henceforth), within which the restricted partition function is written as

$$\mathcal{Z}[\vec{R}] \equiv e^{-\beta\mathcal{H}^{\mathrm{eff}}[\vec{R}]} = e^{-\beta\mathcal{H}^p[\vec{R}]} \times \int \mathcal{D}q(x)$$

$$\times \exp\left\{-\frac{1}{2}\int\frac{dx}{a}\frac{[q(x)-q_0]^2}{(\delta q)^2}\right.$$

$$\left.-\frac{\ell_B}{2}\int\frac{dx}{a}\frac{dx'}{a}\frac{q(x)q(x')e^{-\kappa|\vec{R}(x)-\vec{R}(x')|}}{\left|\vec{R}(x)-\vec{R}(x')\right|}\right\}. \quad (3)$$

In this equation, the energy cost for the deformations of the polyelectrolyte is characterized by an intrinsic bending energy described by the Hamiltonian

$$\beta\mathcal{H}^p[R] = \frac{\ell_p}{2}\int dx(\partial_x^2\vec{R})^2, \quad (4)$$

and a fluctuating electrostatic self energy. The fluctuating linear charge distribution on the PE is characterized by a Gaussian distribution, with the mean (corresponding to the average renormalized charge density and read off from the exact Fuoss-Katchalsky-Lifson solution for an infinitely long uniformly charged rod [41]) given by $q_0 = a/z\ell_B$, and the variance given by $(\delta q)^2 = z(1 - a/z\ell_B)$ [28]. It should be noted that we have included the effect of a low density of added salt in the above equation by adding a screening term [42]. The salt-free case corresponds to $\kappa = 0$.

III. EFFECTIVE ELASTICITY OF THE POLYELECTROLYTE

We next use the methods of Refs. [29,35], to calculate an effective Hamiltonian from the above Gaussian path integral, perturbatively in the deformation field $\mathbf{r}(x)$. We can rewrite the expression in Eq. (3) above as

$$\mathcal{Z}[\vec{R}] = e^{-\beta\mathcal{H}^p[\vec{R}]-\frac{Lq_0^2}{2a(\delta q)^2}} \times \int \mathcal{D}q(x)$$

$$\times \exp\left\{-\frac{1}{2}\int\frac{dx}{a}\frac{dx'}{a}q(x)M(x,x')q(x')\right.$$

$$\left.+\frac{q_0}{(\delta q)^2}\int\frac{dx}{a}q(x)\right\}, \quad (5)$$

where

$$M(x,x') = \frac{a}{(\delta q)^2}\delta(x-x') + \frac{\ell_B}{2}\frac{e^{-\kappa|\vec{R}(x)-\vec{R}(x')|}}{\left|\vec{R}(x)-\vec{R}(x')\right|}. \quad (6)$$

Functional integration over $q(x)$ then yields

$$\beta\mathcal{H}^{\mathrm{eff}} = \beta\mathcal{H}^p[\vec{R}] + \frac{Lq_0^2}{2a(\delta q)^2} + \frac{1}{2}\ln\det\{M(x,x')\}$$

$$-\frac{1}{2}\frac{q_0^2}{(\delta q)^4}\int\frac{dx}{a}\frac{dx'}{a}M^{-1}(x,x'). \quad (7)$$

Now we can write

$$M(x,x') = M_0(x-x') + \delta M(x,x'), \quad (8)$$

or alternatively in Fourier space

$$M(k,k') = 2\pi\delta(k+k')M_0(k) + \delta M(k,k'), \quad (9)$$

in which

$$M_0(k) = \frac{a}{(\delta q)^2} - \ell_B\ln[(k^2+\kappa^2)a^2], \quad (10)$$

and expand Eq. (7) in powers of δM. To the leading order, this yields

$$\beta\mathcal{H}^{\mathrm{eff}} = \beta\mathcal{H}^p + \beta\mathcal{F}_0 + \frac{1}{2}\,\mathrm{tr}(M_0^{-1}\delta M)$$

$$+\frac{1}{2}\frac{q_0^2}{(\delta q)^4}\frac{\delta M(k=0,k'=0)}{[M_0(k=0)]^2}. \quad (11)$$

In the above equation, the trace term is an attractive fluctuation–induced effective free energy, and the term proportional to q_0^2 is a repulsive electrostatic (self-) free energy. The constant term $\beta\mathcal{F}_0$ is independent of the deformations, and thus plays no role in the effective elasticity of the chain. It will be neglected henceforth.

Using the definition of M [Eq. (6)], and the expansion about the rodlike configuration, we find to the leading order

$$\delta M(k,-k) = \int\frac{dp}{2\pi}|\mathbf{r}(p)|^2\left\{\frac{a}{2(\delta q)^2}p^2 - \ell_B p^2\ln[(k^2+\kappa^2)a^2]\right.$$

$$-\frac{\ell_B}{2}(k^2+\kappa^2)\ln[(k^2+\kappa^2)a^2]$$

$$+\frac{\ell_B}{4}[(p+k)^2+\kappa^2]\ln[(p+k)^2a^2+(\kappa a)^2]$$

$$\left.+\frac{\ell_B}{4}[(p-k)^2+\kappa^2]\ln[(p-k)^2a^2+(\kappa a)^2]\right\}. \quad (12)$$

We can then use the expressions for $M_0(k)$ [Eq. (10)] and $\delta M(k,-k)$ [Eq. (12)] and put them into Eq. (11) to find the effective Hamiltonian. We find

$$\beta\mathcal{H}^{\mathrm{eff}}[\mathbf{r}(x)] = \frac{1}{2}\int\frac{dk}{2\pi}\,\mathcal{E}(k)\,|\mathbf{r}(k)|^2 + O(r^4), \quad (13)$$

where

$$\mathcal{E}(k) = \ell_p k^4$$

$$+\frac{q_0^2\ell_B}{2a^2}\left\{\frac{(k^2+\kappa^2)\ln[(k^2+\kappa^2)a^2]-\kappa^2\ln[(\kappa a)^2]}{\left[1+2\left(\frac{\ell_B}{a}\right)(\delta q)^2\ln\left(\frac{1}{\kappa a}\right)\right]^2}\right\}$$

$$-\frac{\ell_B}{2a}(\delta q)^2\int\frac{dp}{2\pi}\left\{\frac{(p^2+\kappa^2)\ln[(p^2+\kappa^2)a^2]}{1-\left(\frac{\ell_B}{a}\right)(\delta q)^2\ln[(p^2+\kappa^2)a^2]}\right.$$

$$\left.-\frac{[(k+p)^2+\kappa^2]\ln[(k+p)^2a^2+(\kappa a)^2]}{1-\left(\frac{\ell_B}{a}\right)(\delta q)^2\ln[(p^2+\kappa^2)a^2]}\right\} + \tau k^2. \quad (14)$$

3

The above expression for the elastic kernel consists of four different contributions:

(i) The intrinsic rigidity of the polyelectrolyte, which has a regular k^4 dependence corresponding to curvature elasticity.

(ii) A repulsive contribution corresponding to electrostatic stiffening of the polyelectrolyte. This is a generalization of the wave vector dependent rigidity first introduced by Barrat and Joanny [3,43], and has a non-analytical k dependence for $\kappa = 0$. (In fact, one can simply recover their formula by setting $(\delta q)^2 = 0$.)

(iii) A fluctuation–induced attractive term that competes with the previous two contributions and tends to soften the polyelectrolyte.

(iv) A term corresponding to line tension renormalization with a k^2 dependence. In general, one can show that such a term should be absent since the rotational symmetry of the original Hamiltonian for a polyelectrolyte requires $\mathcal{E}(k)/k^2 \to 0$ in the limit $k \to 0$ [44]. Since the other terms in Eq. (14) above have a non-vanishing limit as $k \to 0$, one can simply tune τ in such a way that the overall line tension vanishes in that limit [45].

We now examine two limiting cases of the above result in more details.

A. Salt-free solution

The salt-free case is relevant to situations in which the screening length is much larger than the length of the polyelectrolyte, i.e., for $\kappa^{-1} \gg L$. Also in this limit the deformation energy is a non-analytic function of k, and taking the $\kappa = 0$ limit of Eq. (14) requires some care.

$$\mathcal{E}(k) = \frac{\left(\frac{q_0^2}{a^2}\right)\ell_B\,k^2 \ln\left[\left(\frac{k}{k_0}\right)^2 + 1\right]}{2\left[1 + 2(\delta q)^2\left(\frac{\ell_B}{a}\right)\ln\left(\frac{L}{a}\right)\right]^2} - B_1|k|^3 + \ell_p k^4,$$

(15)

with $k_0 \ll \pi/L$ being a cutoff which in the absence of screening is required for a polyelectrolyte [46]. Note that $\partial_{k^2}\mathcal{E}(k)|_{k\to 0} = 0$ to ensure the rotational symmetry, and that Eq. (15) is not just the first few terms in a low-k expansion. The constant B_1 is

$$B_1 = \int_0^{L/a} \frac{dx}{4\pi} \frac{(1+x^2)\ln\left|\frac{x^2}{x^2-1}\right| - 2x\ln\left|\frac{x+1}{x-1}\right| + 3}{\frac{(a/\ell_B)}{2(\delta q)^2} + \ln\left(\frac{L/a}{x}\right)}.$$

(16)

The integral B_1 very slowly depends on $(\delta q)^2(\ell_B/a)$ for typical values, and can be best approximated as $B_1 \simeq c_1/\ln^2\left(\frac{L}{a}\right)$ with $c_1 \simeq 0.101$.

The spectrum of the deformation modes in Eq. (15) consists of an electrostatic repulsion term (that yields the familiar spectrum of a flexible polyelectrolyte in the limit $(\delta q)^2 = 0$ [44,47]). The fluctuation-induced attraction reduces the energy cost, and could even lead to an instability at shorter length scales [48]. The rigidity term $\ell_p k^4$ is the largest power of k included in Eq. (15) and ensures stability at the shortest scales. A negative value of $\mathcal{E}(k)$ for any k indicates a linear instability; the onset of which can be tracked by finding the point when when the minimum of the spectrum, determined from $d\mathcal{E}(k)/dk = 0$, hits the line $\mathcal{E}(k) = 0$. This corresponds to the criterion $\ell_p = \ell_p^c$, where the critical persistence length ℓ_p^c is given by Eq. (1) above, with

$$\Delta_{\rm sf} = \frac{c_1^2}{\ln^2\left(\frac{L}{a}\right)\ln\left[\frac{c_1}{2\ell_p k_0 \ln^2(L/a)}\right]}.$$

(17)

For $\ell_p < \ell_p^c$, there is domain of unstable modes for $k_- < k < k_+$, where

$$k_\pm = \frac{c_1}{2\ell_p \ln^2(L/a)}\left[1 \pm \sqrt{1 - \ell_p/\ell_p^c}\right].$$

(18)

The spectrum of modes given by Eq. (15) is plotted in Fig. 4. To determine the effect of the unstable modes on the conformation of the polyelectrolyte, we should compare the wave vectors with π/L. There are three possibilities: (i) For $k_+ < \pi/L$, the unstable modes cannot be accessed and the polyelectrolyte has an *extended* structure. (ii) For $k_- < \pi/L < k_+$, long wavelength modes have negative energy. Their unstable growth is likely to lead to the collapse of the whole chain. (iii) For $\pi/L < k_-$, the longest wavelength ($\sim \pi/L$) are stable, but there is a range of unstable wavelengths. While linear stability cannot determine the eventual state of the polyelectrolyte, the presence of a finite length scale could well be the precursor of a *necklace* structure.

The corresponding phase diagram is depicted in Fig. 2. A suggested boundary between the collapsed and other phases is obtained from $k_\pm = \pi/L$, as

$$\frac{\ell_p}{a} = \frac{\left(\frac{L}{a}\right)}{\pi \ln^2\left(\frac{L}{a}\right)}\left[c_1 - \frac{\left(\frac{L}{a}\right)\ln\left(\frac{\pi}{Lk_0}\right)}{4\pi z^4\left(\frac{\ell_B}{a}\right)^3\left(1 - \frac{a}{z\ell_B}\right)^2}\right], \quad (19)$$

and has a nearly parabolic shape, leading to reentrant extended states.

B. Added-salt

The addition of salt leads to a finite screening length κ^{-1}, and for $\kappa^{-1} \ll L$, the spectrum $\mathcal{E}(k)$ given by Eq. (13) is an analytic function of k with a well defined power expansion. The lowest order term in the expansion is proportional to k^4, whose coefficient can be regarded as the 'effective rigidity' of the polyelectrolyte, and given by

$$L_p = \ell_p + \frac{1}{4}\frac{q_0^2\ell_B}{\left[1 + 2(\delta q)^2\left(\frac{\ell_B}{a}\right)\ln\left(\frac{1}{\kappa a}\right)\right]^2(\kappa a)^2} - \frac{B_2}{2\kappa},$$

(20)

in which

$$B_2 = \int_0^{1/\kappa a} \frac{dx}{4\pi} \frac{11x^4 + 2x^2 - 1}{(x^2+1)^3 \left\{ \frac{(a/\ell_B)}{(\delta q)^2} + \ln\left[\frac{(1/\kappa a)^2 + 1}{x^2 + 1} \right] \right\}}. \quad (21)$$

Again, the integral B_2 has a very slow dependence on $(\delta q)^2 (\ell_B/a)$ for typical values, and can be best approximated as $B_2 \simeq c_2 / \ln\left(\frac{1}{\kappa a}\right)$ with $c_2 \simeq 0.288$, leading to the effective persistence length given in Eq. (2). It is interesting to note that a similar result has been predicted for stiff polyampholytes [50].

Interestingly, Eq. (20) reproduces the OSF electrostatic persistence length in the limit $(\delta q)^2 = 0$ [36], with a reduced charge density q_0. Upon including the counterion fluctuations, $(\delta q)^2 \neq 0$, there is a reduction of the repulsive term, as well as the appearance of an attractive term. As a result, the polyelectrolyte 'rigidity' (effective persistence length) can become very low and even have negative values which we take as indicating a conformational instability (collapse). Using this criterion ($L_p = 0$), we obtain the phase diagram shown in Fig. 4, which like the salt–free case, has a nearly parabolic shape, with a maximum that yields the critical persistence length given in Eq. (1) with $\Delta_{\rm as} = c_2^2 \simeq 0.0829$. Once more, its shape suggests that the instability is a reentrant effect. Note that the critical persistence length for the case with added salt is larger than the salt–free case.

IV. DISCUSSION

The above results can be related to some experimental findings concerning polyelectrolyte elasticity in the presence of multivalent counterions. In a direct single DNA manipulation experiment, Baumann *et al.* used a force-measuring optical tweezer to determine the elastic properties of λ-bacteriophage DNA in the presence of multivalent counterions [51]. They observed that the apparent persistent length of the DNA (extracted from force–extension curves using the wormlike chain model) goes down to as low as 250-300 $\mathring{A}$, which is well below the fully saturated high salt value 450-500 $\mathring{A}$ (denoted as ℓ_p above) in the presence of multivalent ions [51]. This is in agreement with the generalised effective persistence length given in Eq. (2). There may be of course, other contributions to the effective persistence length coming from other types of charge correlations.

Flexible polyelectrolytes have also been shown to collapse in the presence of divalent ions [6]. Interestingly, there is evidence that for sodium polyacrylate chains the collapsed states are not always compact spherical shapes at *lower* salt concentrations [6] and may have cigar-like or pearl-necklace shapes. This is in agreement with the results we obtained in the salt-free regime.

We now conclude with a qualitative summary of the nature of the results, and the range of their validity. From dimensional analysis, it is easy to show that *unscreened* Coulomb interactions make a contribution of $\ell_B(k/a)^2$ to the rigidity spectrum $\mathcal{E}(k)$. In the PB solution, due to charge condensation the strength of this term is reduced by a factor of $q_0^2 = (a/z\ell_B)^2$. If the charge density on the polyelectrolyte is allowed to fluctuate, it is further reduced, and the Coulomb rigidity goes down by a factor of $(\delta q)^4 (\ell_B/a)^2 \ln^2(L/a)$, with $(\delta q)^2 = z(1 - q_0)$. However, these reductions do not change the overall sign which still prefers a rodlike structure. An attractive (destabilizing) contribution is generated by fluctuation-induced interactions, which are typically independent of microscopic parameters, and hence make a contribution of $-k^3$ to $\mathcal{E}(k)$. In comparison to the leading Coulomb contribution, the latter corrections become important at *short scales* of order of a^2/ℓ_B. We thus may well question the applicability of continuum formulations to describe such a short-distance instability. In hindsight, the phase diagrams of Fig. 2 and Fig. 3 indicate that the prefactors involved in softening of the residual repulsion conspire to make the actual instability lengths quite large ($\sim z^4\ell_B^3/a^2$), and thus the continuum formulation should hold for a large portion of these phase diagrams [52].

Another potential concern is the choice of the charge variance $(\delta q)^2$. While our approach ignores the finite size of the counterions and allows for a large number of them to be condensed in the vicinity of a single charged group on the polyelectrolyte, there are other models that have restricted this number to one [8,25]. Given the relatively large radius of DNA and actin as compared to the size of typical counterions, the restriction of this number to one seems to be artificial, as it leads erroneously to zero charge fluctuations at complete condensation. Nonetheless, we believe that considering the finite size of the counterions in a realistic way will certainly be a worthwhile improvement of our approach. Finally, the instability analysis performed here only provides us with information concerning the onset of a conformational change. The final structure of the collapsed chain is naturally beyond this linear stability analysis [11,53].

It is known experimentally that different counterions with the same valence may behave differently as collapsing agents. The difference is usually attributed to modifications in the microscopic structure of the polyelectrolyte that take place upon binding of the counterions [11]. It is thus plausible that the microscopic features that distinguish between different counterions with the same electrostatic properties can be encoded in a single parameter, the microscopic persistence length, which normally depends only on the local microscopic structure of the polyelectrolyte backbone.

5

[1] G.S. Manning, J. Chem. Phys. **51**, 954 (1969).
[2] F. Oosawa, Biopolymers **6**, 134 (1968); F. Oosawa, *Polyelectrolytes* (Marcel Dekker, New York, 1971).
[3] J.L. Barrat and J.F. Joanny, Adv. Chem. Phys. **94**, 1 (1996).
[4] M. Le Bret, J. Chem. Phys. **76**, 6243 (1982); M. Fixman, J. Chem. Phys. **76**, 6346 (1982).
[5] M. Delsanti, J.P. Dalbiez, O. Spalla, L. Belloni, and M. Drifford, ACS Symp. Ser. **548**, 381 (1994).
[6] R. Schweins and K. Huber, Eur. Phys. J. **E 5**, 117 (2001); Y. Ikeda, M. Beer, M. Schmidt and K. Huber, Macromolecules **31**, 728 (1998); K. Huber, J. Phys. Chem. **97**, 9825 (1993). There are also similar observations in: B.L. Smith, D.R. Gallie, H. Le, and P.K. Hansma, Journal of Structural Biology **119**, 109 (1997).
[7] M.J. Stevens and K. Kremer, Phys. Rev. Lett. **71**, 2228 (1993); J. Chem. Phys. **103**, 1669 (1995).
[8] P. Gonzalez-Mozuelos and M. Olvera de la Cruz, J. Chem. Phys. **103**, 3145 (1995); M. Olvera de la Cruz, L. Belloni, M. Delsanti, J.P. Dalbiez, O. Spalla, M. Drifford, J. Chem. Phys. **103**, 5781 (1995).
[9] N.V. Brilliantov, D.V. Kuznetsov, and R. Klein, Phys. Rev. Lett. **81**, 1433 (1998).
[10] H. Schiessel and P. Pincus, Macromolecules **31**, 7953 (1998).
[11] V.A. Bloomfield, Biopolymers **31**, 1471 (1991); V.A. Bloomfield, Curr. Opin. Struct. Biol. **6**, 334 (1996).
[12] J.X. Tang, S. Wong, P. Tran, and P.A. Janmey, Ber. Bunsen-Ges. Phys. Chem. **100**, 1 (1996); J.X. Tang, T. Ito, T. Tao, P. Traub, and P.A. Janmey, Biochemistry **36**, 12600 (1997).
[13] A.P. Lyubartsev, J.X. Tang, P.A. Janmey, and L. Nordenskiold, Phys. Rev. Lett. **81**, 5465 (1998).
[14] M.J. Stevens, Phys. Rev. Lett. **82**, 101 (1998).
[15] G.S. Manning, Biopolymers **19**, 37 (1980); G.S. Manning, Cell Biophys. **7**, 57 (1985).
[16] I. Rouzina, and V. A. Bloomfield, Biophys. J. **74**, 3152 (1998).
[17] T. T. Nguyen, I. Rouzina, and B. I. Shklovskii, Phys. Rev. E **60**, 7032 (1999).
[18] R. Golestanian, M. Kardar, and T.B. Liverpool, Phys. Rev. Lett. **82**, 4456 (1999).
[19] P.L. Hansen, R. Podgornik, D. Svensek, and V. A. Parsegian, Phys. Rev. E **60**, 1956 (1999).
[20] G. Ariel and D. Andelman, preprint cond-mat/0112337.
[21] I. Rouzina and V.A. Bloomfield, J. Phys. Chem. **100**, 9977 (1996).
[22] N. Gronbech-Jensen, R.J. Mashl, R.F. Bruinsma, and W.M. Gelbart, Phys. Rev. Lett. **78**, 2477 (1997)
[23] B.I. Shklovskii, Phys. Rev. Lett. **82**, 3268 (1999).
[24] J.J. Arenzon, J.F. Stlick, and Y. Levin, Eur. Phys. J. B **12**, 79 (1999).
[25] F.J. Solis and M. Olvera de la Cruz, Phys. Rev. E **60**, 4496 (1999).
[26] A.A. Kornyshev, and S. Leikin, J. Chem. Phys. **107**, 3656 (1997); Biophys. J. **75**, 2513 (1998); Phys. Rev. Lett. **82**, 4138 (1999); Phys. Rev. Lett. **84**, 2537 (2000).
[27] R. Podgornik and V.A. Parsegian, Phys. Rev. Lett. **80**, 1560 (1998).
[28] B.-Y. Ha and A.J. Liu, Phys. Rev. Lett. **79**, 1289 (1997); Phys. Rev. Lett. **81**, 1011 (1998); Physica A **259**, 235 (1998); Phys. Rev. E **58**, 6281 (1998); Europhys. Lett. **46**, 624 (1999); Phys. Rev. E **60**, 803 (1999).
[29] M. Kardar and R. Golestanian, Rev. Mod. Phys. **71**, 1233 (1999).
[30] B.I. Shklovskii, Phys. Rev. E **60**, 5802 (1999).
[31] R. Messina, C. Holm, and K. Kremer, Phys. Rev. Lett. **85**, 872 (2000); Europhys. Lett. **51**, 461 (2000).
[32] J. Ray and G.S. Manning, Langmuir **10**, 2450 (1994); Macromolecules **30**, 5739 (1997); Macromolecules **33**, 2901 (2000);
[33] A.G. Moreira and R.R. Netz, Phys. Rev. Lett. **87**, 078301 (2001); R.R. Netz, Eur. Phys. J. E **5**, 557 (2001); R.R. Netz, in *Electrostatic Effects in Soft Matter and Biophysics*, C. Holm et al. (eds.), pp. 367-408 (Kluwer, Amsterdam, 2001).
[34] A.W.C. Lau, P. Pincus, D. Levine, and H.A. Fertig, Phys. Rev. E **63**, 051604 (2001).
[35] H. Li and M. Kardar, Phys. Rev. Lett. **67**, 3275 (1991); Phys. Rev. A **46**, 6490 (1992); R. Golestanian and M. Kardar, Phys. Rev. Lett. **78**, 3421 (1997); Phys. Rev. A **58**, 1713 (1998).
[36] T. Odijk,, J. Polym. Sci. **15**, 477 (1977); J. Skolnick and M. Fixman, Macromolecules **10**, 944 (1977).
[37] A.W.C. Lau and P. Pincus, Phys. Rev. Lett. **81**, 1338 (1998); B.-Y. Ha, Phys. Rev. E **64**, 031507 (2001); Phys. Rev. E **64**, 051902 (2001); R.R. Netz, Phys. Rev. E **64**, 051401 (2001).
[38] R. Golestanian, Europhys. Lett. **36**, 557 (1996).
[39] J. Pelta, D. Durand, J. Doucet, and F. Livolant, Biophysical Journal **71**, 48 (1996); J. Pelta, F. Livolant, and J.L. Sikorav, Journal of Biological Chemistry **271**, 5656 (1996); E. Raspaud, M. Olvera de la Cruz, J.L. Sikarov, and F. Livolant, Biophysical Journal **74**, 381 (1998); M. Saminathan, T. Antony, A. Shirahata, L. Sigal, T. Thomas, and T.J. Thomas, Biochemistry **38**, 3821 (1999).
[40] T.T. Nguyen, I. Rouzina, and B.I. Shklovskii, e-print cond-mat/9908428.
[41] R.M. Fuoss, A. Katchalsky, and S. Lifson, Proc. Natl. Acad. Sci. USA **37**, 579 (1951).
[42] The density of the salt n should be low enough not to smear out the condensation. The requirement of the mass contrast to be substantial, yields $n \ll z(1 - a/z\ell_B)/(aS)$, where S is the cross sectional area of the polyelectrolyte.
[43] J.L. Barrat and J.F. Joanny, Europhys. Lett. **24**, 333 (1993).
[44] Y. Kantor and M. Kardar, Europhys. Lett. **9**, 53 (1989).

[45] In order to actually calculate τ from the path integral formulation correctly, and prove that it does cancel the other contributions to the line tension as rotational symmetry requires, one should construct a more delicate field theory with invariant measures, etc., which was not the aim of the present work. For a related discussion in the case of fluid membranes see: W. Cai, T.C. Lubensky, P. Nelson, and T. Powers, J. Phys. II France **4**, 931 (1994).

[46] For wavelength such that $k \gg k_0$ we can approximate $\ln[(k/k_0)^2 + 1]$ by $2\ln(k/k_0)$. Although, strictly speaking, one should finally take the limit $k_0 \to 0$, it is sufficient for practical purposes that k_0 is small enough such that $\sin(k_0 L) \simeq k_0 L$. With this in mind, we have selected $k_0 = 10^{-3}\pi/L$ for the phase diagram of Fig. 2.

[47] H. Li and T.A. Witten, Macromolecules **28**, 5921 (1995).

[48] The repulsive part of the spectrum comes from a pair potential of the form $(a/z\ell_B)^2/z^2\ell_B r$, while the attractive fluctuation-induced part can be obtained from a $-1/r^2$ pair potential. This leads to a short length scale instability for $r < z^4(\ell_B/a)^2\ell_B$.

[49] A necklace structure for randomly charged polymers was introduced in Y. Kantor and M. Kardar, Europhys. Lett. **27**, 643 (1994); Y. Kantor and M. Kardar, Phys. Rev. **E51**, 1299 (1995). Its applicability to uniformly charged polyelectrolytes is discussed in A.V. Dobrynin, S.P. Obukhov, and M. Rubinstein, Macromolecules **29**, 2974 (1996).

[50] B.-Y. Ha and D. Thirumalai, J. Phys. II (France), **7**, 887 (1997).

[51] C.G. Baumann, S.B. Smith, V.A. Bloomfield, and C. Bustamante, Proc. Natl. Acad. Sci. USA **94**, 6185 (1997).

[52] From these arguments, it is clear that counterions with higher valence z are much more effective in collapsing the polyelectrolytes. Nonetheless, Eq.(1) does not rule out the possibility of collapse for monovalent counterions, provided that the polyelectrolyte has a low enough microscopic persistence length.

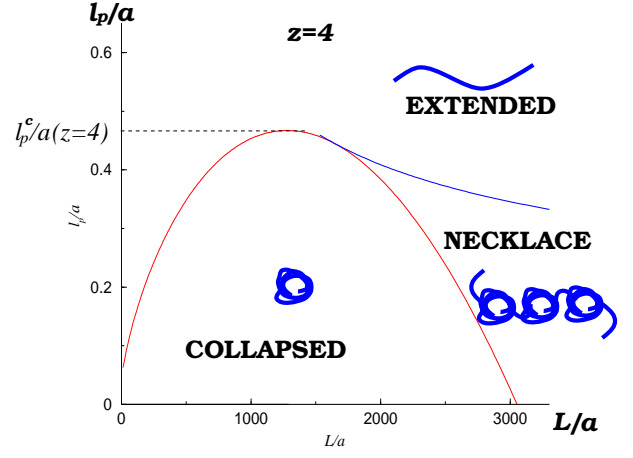[53] S.Y. Park, D. Harries, and W. M. Gelbart, Biophys. J. **75**, 714 (1998).

FIG. 2. Phase diagram for the salt-free case, for $z = 4$. The parameters $a = 1.7\mathring{A}$, and $k_0 = 10^{-3}\pi/L$ are used.
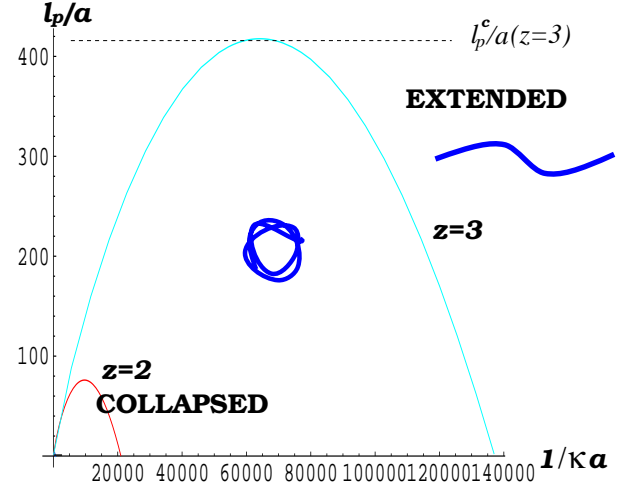

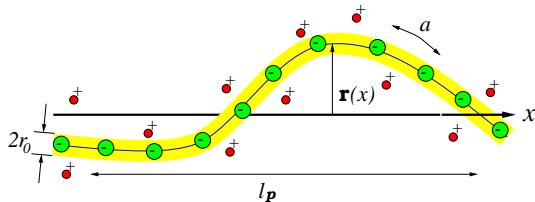FIG. 3. Phase diagram for the added-salt case, for different values of the counterion valence z.

FIG. 1. Schematic of the extended polyelectrolyte parametrized by $R(x) = (x, \mathbf{r}(x))$.
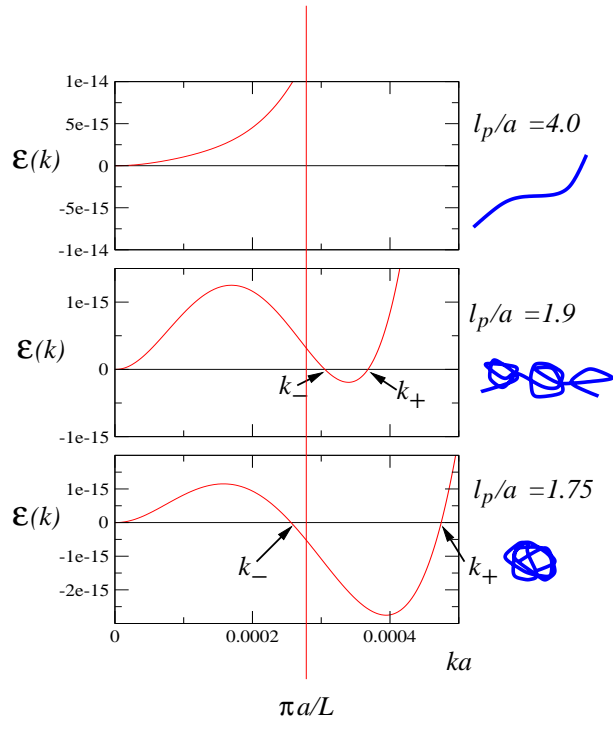
FIG. 4. The energy spectrum $\mathcal{E}(k)$ for the salt-free regime showing the unstable modes.

$\mathcal{E}(k)$

$l_p/a = 4.0$

$\mathcal{E}(k)$

$l_p/a = 1.9$

k_- k_+

$\mathcal{E}(k)$

$l_p/a = 1.75$

k_- k_+

ka

$\pi a/L$